Electrosynthesis and optical modeling of ZnO nanostructures

Narges Ajami[a,*], Ali Ehsani [b], Ferydon Babaei [c], Ashraf Heidaripour[d]

[a]*Department of Chemistry, Payame Noor University, P.O. BOX 19395-3697 Tehran, Iran*

[b] *Department of Chemistry, Faculty of science, University of Qom, P.O. BOX 37185-359, Qom, Iran*

[c]*Department of Physics, Faculty of science, University of Qom, P.O. BOX 37185-359, Qom, Iran*

[d]*Department of Chemistry, Faculty of Science, K. N. Toosi University of Technology, Tehran, Iran*

Abstract

Optical modeling was applied for obtaining absorbance spectra and band gap values for different morphology of ZnO semiconductor. In optical modeling, the relative permittivity scalars of zinc oxide coral like nanorods were calculated using the Bruggeman homogenization formalism. ZnO nano rods (ZONRs) as a nucleus layer were fabricated on the Indium Tin Oxide (ITO) by chronoamperometry (CA) in aqueous solution containing different concentration of zinc nitrate. Reduction of nitrate anion is a good resource for hydroxyl ion that with zinc anion results ZnO. The orientation and morphology of both the nucleus layer and successive coral like ZONRs were analyzed using X-ray diffraction (XRD).

Keywords: Optical modeling; ZnO; chronoamperometry; coral-like nanostructure.

Introduction

Zinc oxide (ZnO) is an n-type semiconductor with a wide bandgap of 3.2 eV and bulk exciton binding energy 60meV [1] with transparent and conductive properties. At ambient conditions, ZnO has the wurtzite structure. The band structure of ZnO calculated with FP- LAPW method shows that ZnO with wurtizite structure has a direct band gap [2]. The ZnO films are employed for several applications due to their electrical, optical, and acoustic characteristics [2], ultraviolet emitting diodes, Piezoelectric devices, sensors, and solar cells [1]. ZnO thin films have been prepared by different techniques such as spray pyrolysis, thermal evaporation, sol gel, pulsed laser deposition, molecular beam epitaxy (MBE), sputtering [3,4] and electrochemical deposition [5,6,7]. Electrosynthesis is an appropriate process, which is known for micro and nano-structuring of the metals, polymers and semiconductors which used in our previous works for electrosynthesis of conducting polymer with different morphology [8-12]. In electrochemical technique, ZnO nanoseeds were prepared by using zinc nitrate applying cathodic potential within potential modulation method (Pulse) [1] and cyclic voltammetry (CV) [7]. During this process, nitrate is reduced to nitro and hydroxide, the hydroxide with Zn^{+2} form $\mathbf{Zn\,(OH)}_{ad}^{+}$ and finally ZnO is formed [1]. The

*Corresponding author: Narges Ajami

Tel: +98 (021) 88940006, Fax: +98 (021) 88940007

E-mail: n_ajami@pnu.ac.ir

ZONRs were hydrothermally grown directly onto the substrate, using an equimolar aqueous solution of zinc nitrate and hexamethylenetetramine [7,13]. Scanning electron microscopy (SEM) shows that ZnO film iscompacted with hexagonal-shaped crystal [1,7]. Meanwhile, ZnO surface as a polar crystal is either positively charged or negatively charged. The optimized {0 0 1} surface obtained with XRD has roughly a 60% higher cleavage energy than the nonpolar {1 0 0} and {1 1 0} faces. ZnO has a dipole moment along (0 0 1) direction. These properties suggest that the c axis is the fastest growth direction and the ZnO {0 0 1} has the highest energy of the low index surface and ZnO grows along this direction easily [7, 14]. In this work, Optical modeling and the Bruggeman homogenization formalism were applied for obtaining absorbance spectra and band gap values for different morphology of ZnO semiconductor.

Experimental

The ITO film was purchased from Dyesol. Materials Zn (NO3)2.6H2O, hexamethylenetetramine (C6H12N4) with commercial name of thiamine were used without more purification. All materials were of analytical grade (Merck). All electrochemical measurements were carried out in a conventional three electrodes cell powered by a Metrohm Autolab (PG STAT-12/30/302). The clean ITO glass sheets with active area of 1.0×1.5 cm2 and resistivity of 22Ω have been used as a working electrode (cathode). A large area of Pt foil was used as a counter electrode and an Ag/AgCl electrode (KCl saturated) as reference electrode. The morphologies of the ITO/ZONRs obtained were analyzed using field emission scanning electron

micro analyzer model KYKY-EM3200. Crystalline morphology is investigated by XRD using Shimadzu (XRD-6000) with λ= 1.54060nm. The ZnO nucleus layers were electrodeposited via CA in zinc nitrate aqueous solution with different concentration of 0.001, 0.01 and 0.1M which are presented with sample 1, 2 and 3, respectively. The applied potential was confirmed through -0.803V / Ag/AgCl during 100s. The substrates were covered with ZnO nucleus layer and plunged in an aqueous solution with equimolar of zinc nitrate and thiamine (growth system) to grow ZnO within different times, 45 and 90min. The temperature of growth system was 90˚C. Subsequently, the grown films were thoroughly rinsed with DI water and allowed to be dried at room temperature. The grown ZnO in the growth system were named sample 4 (45 min) and sample 5 (90 min).

Optical modeling

Consider the region $0 \leq z \leq d$ be occupied by coral like nanorods (Figure 1) while the regions $z \leq 0$ and $z \geq d$ are vacuous. Suppose an arbitrarily polarized plane wave is normally incident (axial excitation) on the chosen structure from $z \leq 0$. The phasors of incident, reflected and transmitted electric fields are given as [15]:

$$\begin{cases} \underline{E}_{inc}(\underline{r}) = [a_s \underline{u}_y - a_p \underline{u}_x] e^{i K_0 z}, & z \leq 0 \\ \underline{E}_{ref}(\underline{r}) = [r_s \underline{u}_y + r_p \underline{u}_x] e^{-i K_0 z}, & z \leq 0 \\ \underline{E}_{tr}(\underline{r}) = [t_s \underline{u}_y - t_p \underline{u}_x] e^{i K_0 (z-d)}, & z \geq d \end{cases}$$
(1)

Where (a_s, a_p), (r_s, r_p) and (t_s, t_p) are the amplitudes of incident plane wave, an reflected and transmitted waves with S- or P- polarizations, $K_0 = \omega\sqrt{\mu_0\varepsilon_0} = 2\pi/\lambda_0$ is the free space wave number, λ_0 is the free

space wave length, $\varepsilon_0 = 8.854 \times 10^{-12} Fm^{-1}$, $\mu_0 = 4\pi \times 10^{-7} \ Hm^{-1}$ are the permittivity and permeability of free space (vacuum) and $\underline{u}_{x,y,z}$ are the unit vectors in Cartesian coordinates system.

The reflectance and transmittance amplitudes can be obtained using the continuity of the tangential components of electrical and magnetic fields at interfaces and solving the algebraic matrix equation [16]:

$$\begin{bmatrix} t_s \\ t_p \\ 0 \\ 0 \end{bmatrix} = [\underline{\underline{K}}]^{-1}.[\underline{\underline{M}}].[\underline{\underline{K}}].\begin{bmatrix} a_s \\ a_p \\ r_s \\ r_p \end{bmatrix} \qquad (2)$$

The different terms and parameters of this equation are given in detail by Lakhtakia [15]. In our work, the absorbance for natural light is

$$A = -Log[\frac{T_S + T_P}{2}]$$

where

$$T_i = \sum_{j=s,p} T_{ji} \ ; T_{i,j} = \left| \frac{t_i}{a_j} \right|^2 \ ; i, j = s, p \ \ .$$
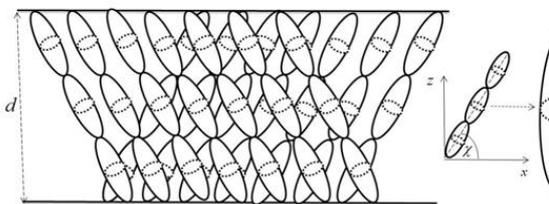
Figure 1. Schematic of the boundary-value problem for optical modeling
The angle of rise nanorods is χ ; c, a, b are semi major axis and small half-axes of ellipsoids, respectively.

Result and discussion
Figure 2 illustrates the SEM images of sample 3(a), and 4(b) and 5(c). It is obvious that ZONRs have grown on the nucleus layer obliquely in a manner that coral- like nanorods were formed. As

shown, ZONRs have dimension of 15.62 nm diameter and 1.08 µm lengths.
Figure 3 shows the XRD information of the deposited material on the ITO. Corresponding to Figure 3 a, b and c are related to sample 3, 4 and 5, respectively.

In the case of sample 3 (Figure 3a), several different phases are composed and these phases are assigned as ZnO [1]. Though several phases of ZnO are observed within range from 2theta= 20° to 70°, especially two phases in ZnO (100) at 27.34° and (101) at 38.66° are dominant on the ITO substrate. Also other phases with weaker intensity exist as (102), (110) and (103) that are concerned to ZnO wurtzite structure.
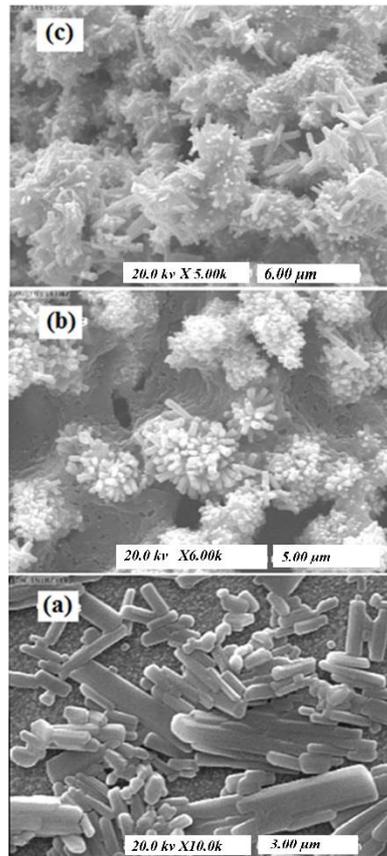
Figure 2. SEM image of (a) nucleus layer fabricated on the ITO by CA technique and (b) a single nanorode with dimension of 15 nm diameter and 1.08 µm lengths
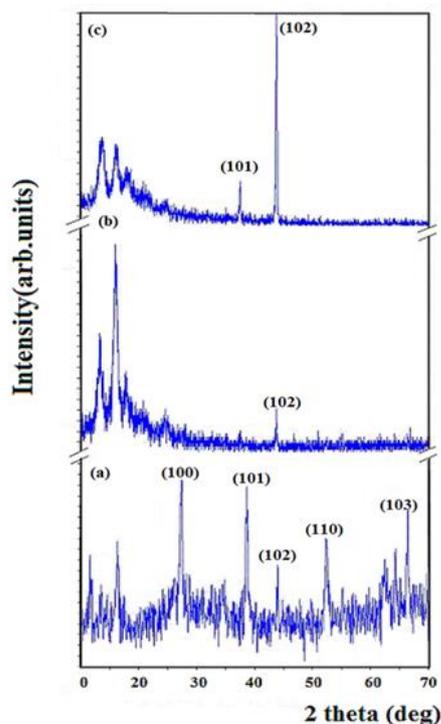
Figure 3. XRD of the nucleus layer on the ITO prepared by CA technique (a), sample grown during (b) 45min and (c) 90min in growth setup

These data admit growth in direction of x that result horizontal growth. Within range from 2theta=0° to 20° some wide peaks are observed that exist in all XRDs before and after growth that they could be related to ITO substrate [7,17]. As it is clear in Figure 3b (XRD related to sample 4), the preferred orientation is along (102). The uniform crystallites cause higher density of nuclei on the nucleus surface in the (102) direction so rods stand completely oblique. The same way of growth exists for XRD of sample 5, Figure 3c, that crystallizing occurs in preferred orientation (102). A peak with weaker intensity exists in direction of (101). This kind of growth results coral-like structures. Therefore, XRD results are in good agreement with what exists in SEM images. In optical modeling, the relative permittivity scalars of zinc oxide coral-like nanorods were calculated using the Bruggeman homogenization formalism [18-20]. In this formalism, the structure is considered as a two phase composite (vacuum phase and inclusion phase (ZnO). These quantities depend on different parameters, namely, columnar form factor, fraction of zinc oxide (f_{ZnO}), the wavelength of free space and the refractive index. In addition, each column in the structure is considered as a string of identical long ellipsoids(c, a, b are semi major axis and small half-axes of ellipsoids) (Figure 1) [15]. The ellipsoids are considered to be electrically small (i.e. small in a sense that their electrical interaction can be ignored) [21]. Setting the shape factors and will make each ellipsoid resemble a needle with a slight bulge in its middle part. We have extracted the refractive index zinc oxide for homogenization from Ref [22]. Also, we have included the dispersion and dissipation of dielectric function.

The calculated absorbance spectra as a function of wavelength for coral-like nanorods of ZnO from reduction of Zn (NO3)2 solution with concentration of 0.001, 0.01, and 0.1M are depicted in Figure 4.

In our calculation for Figure 4, the experimental structural parameters of thin film, thickness d=20nm, =45° were fixed. For concentration of 0.001, 0.01, and 0.1M of Zn (NO3)2 solution, a=1,b=2,c=10, =0.75; a=1,b=2,c=15, =0.85; a=1,b=2,c=20, =0.95 are respectively considered. Also, the regions of void are simulated as spheres (a=b=c=1). In Figure 4a, it can be seen that as the concentration of solution increases, the edge of absorbance shifts to higher wavelengths. The plots of vs. photon energy are shown in Figure 4b, where (A is absorbance, d is thickness of thin films). It has been observed that

the plots of versus are linear over a wide range of photon energies indicating the direct type of transitions. The intercepts (extrapolations) of these plots (straight lines) on the energy axis give the energy band gaps. The direct band gaps Eg of 0.001M, 0.01M and 0.1M were determined 3.30eV ,3.26eV and 3.22eV, respectively.

The calculations are repeated for 0.1M concentration of Zn (NO3)2 solution for fabrication zinc oxide coral-like nanorods with different time of growth, as are shown in Figure 5. The results showed that as the thickness of thin film increases, the edge of absorbance shifts to higher wavelengths (Figure 5a). This has been seen in Figure 5b as well and we found the direct band gaps Eg of nucleation state (d=20nm), 45 Min (d=45nm) and 90 Min (d=73nm) were determined 3.24 eV, 3.27eVand 3.35eV, respectively.
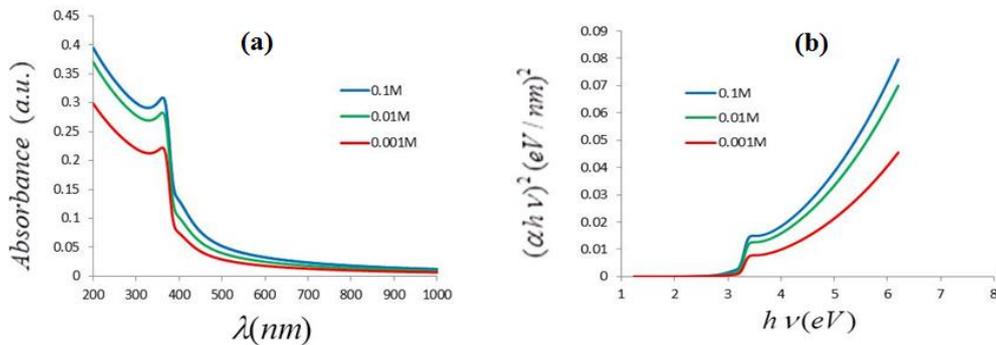
Figure 4. Calculated absorbance and $(\alpha h \nu)^2$ for coral- like nanorods of ZnO from reduction of Zn (NO$_3$)$_2$ solution with concentration of 0.001, 0.01, and 0.1M, (a) absorbance vs. wavelength; (b) $(\alpha h \nu)^2$ vs. photon energy
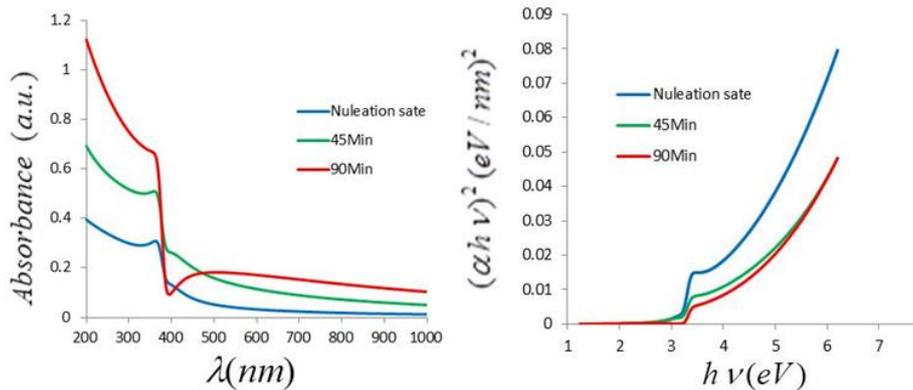
Figure 5. Calculated absorbance and $(\alpha h \nu)^2$ for coral-like nanorods of ZnO from reduction of Zn (NO$_3$)$_2$ solution with concentration of 0.1M at different times of growth, (a) absorbance vs. wavelength; b) $(\alpha h \nu)^2$ vs. photon energy

Conclusion

In this work, we presented Chronoamperometry (CA) technique for fabrication of ZnO nanorods as a nucleus layer on the ITO. The orientation and morphology of both the nucleus layer and grown ZONRs have been analyzed by using SEM images and XRD. Optical modeling was applied for obtaining absorbance

spectra and band gap values for different morphology of ZnOsemiconductor.

In optical modeling, the relative permittivity scalars $\varepsilon_{a,b,c}$ of zinc oxide coral-like nanorods were calculated using the Bruggeman homogenization formalism.

References
[1] J. Lee, and Y. Takb, *Electrochem. Solid-State. Lett.*, **2011**, *4*, 63-65.
[2] W.Y. Liang, A.D. Yoffe, *Phys. Rev. Lett.*, **1968**, *20*, 59-62.
[3] M. Mekhnache, A. Drici, L. SaadHamideche, H. Benzarouk, A. Amara, L. Cattin, J.C. Bernède, M. Guerioune, *Super lattices Microstruct.,* **2011**, *49*, 510-518.
[4] B.T. Tang, Q.X. Yu, H.Y. Lee, C.T. Lee, *Mater. Sci. Eng., B* **2001**, *82*, 259-261.
[5] Z. Chen, Y. Tang, L. Zhang, L. Luo, *Electrochim. Acta.,* **2006**, *51*, 5870-5875.
[6] Y. Hwan Ko, M. Sub Kim, J. Su Yu, *Appl. Surf. Sci.,* **2012**, *259*, 99-104.
[7] Z. Liu, L.E.J. Ya, Y. Xin, *Appl. Surf. Sci.,* **2009**, *255*, 6415-6420.
[8] N. Ajami, N. Bahrami Panah, I. Danaee, *Iran Polym J.*, **2014**, *23*,121-126.
[9] N. Ajami, N. Bahrami Panah, *J.Nanostr. Chem. (JNSC),* **2013**, *76,* 1-5.
[10] A. Ehsani, M.G. Mahjani, M. Bordbar, R. Moshrefi, *Synth. Met.,* **2013**, *165*, 51-55.
[11] A. Ehsani, M.G. Mahjani, M. Jafarian, A. Naeemy, *Electrochim. Acta.,* **2012**, *71*, 128-133.
[12] A. Ehsani, M.G. Mahjani, M. Jafarian, *Synth. Met.*, **2012**, *62*, 199-204.
[13] M. Reinhard, J. Conradt, M. Braun, A. Colsmann, U. Lemmer, Heinz Kaltb, Heinz Kalt, *Synth. Met.,* **2012**, *162*, 1582-1586.
[14] L. Vayssieres, K. Keis, S.E. Lindquist, A. Hagfeldt, *J. Phys. Chem., B* **2001**, *105*, 3350-3352.
[15] A. Lakhtakia, R. Messier, Sculptured thin films, Nano engineered Morphology and Optics (SPIE, USA, **2005**).
[16] V.C. Venugopal, A. Lakhtakia, *Proc. R. Soc. London A ,* **2000**, *456*, 125-161.
[17] G. She, X. Zhang, W. Shi, X. Fan, J.C. Chang, *Electrochem. Commun.,* **2007**, *9*, 2784-2788.
[18] Lakhtakia, A. *Microw. Opt. Technol. Lett.,* **2000**, *24*, 239-244.
[19] F. Babaei, H. Savaloni, *Opt. Commun.,* **2007**, *278*, 221-231.
[20] F. Babaei, H. Savaloni, *J. Mod. Optics,* **2008**, *55*, 1845-1857.
[21] F. Babaei, H. Savaloni, *Opt. Commun.,* **2007**, *278*, 321-328.
[22] Y.C. Liu , J.H. Hsieh , S.K. Tung , *Thin Solid Films.,* **2006**, *510*, 32-38.